Estuarine, Coastal and Shelf Science 89 (2010) 89–96

Contents lists available at ScienceDirect

Estuarine, Coastal and Shelf Science

journal homepage: www.elsevier.com/locate/ecss

Remote sensing of water depths in shallow waters via artificial neural networks

Özçelik Ceyhun*, Arısoy Yalçın

Department of Civil Engineering, Dokuz Eylul University, 35160 Izmir, Turkey

ARTICLE INFO

Article history:
Received 25 November 2009
Accepted 26 May 2010
Available online 2 June 2010

Keywords:
water depth
bathymetry
remote sensing
artificial neural networks

ABSTRACT

Determination of the water depths in coastal zones is a common requirement for the majority of coastal engineering and coastal science applications. However, production of high quality bathymetric maps requires expensive field survey, high technology equipment and expert personnel. Remotely sensed images can be conveniently used to reduce the cost and labor needed for bathymetric measurements and to overcome the difficulties in spatial and temporal depth provision. An Artificial Neural Network (ANN) methodology is introduced in this study to derive bathymetric maps in shallow waters via remote sensing images and sample depth measurements. This methodology provides fast and practical solution for depth estimation in shallow waters, coupling temporal and spatial capabilities of remote sensing imagery with modeling flexibility of ANN. Its main advantage in practice is that it enables to directly use image reflectance values in depth estimations, without refining depth-caused scatterings from other environmental factors (e.g. bottom material and vegetation). Its function-free structure allows evaluating nonlinear relationships between multi-band images and in-situ depth measurements, therefore leads more reliable depth estimations than classical regressive approaches. The west coast of the Foca, Izmir/Turkey was used as a test bed. Aster first three band images and Quickbird pan-sharpened images were used to derive ANN based bathymetric maps of this study area. In-situ depth measurements were supplied from the General Command of Mapping, Turkey (HGK). Two models were set, one for Aster and one for Quickbird image inputs. Bathymetric maps relying solely on in-situ depth measurements were used to evaluate resultant derived bathymetric maps. The efficiency of the methodology was discussed at the end of the paper. It is concluded that the proposed methodology could decrease spatial and repetitive depth measurement requirements in bathymetric mapping especially for preliminary engineering application.

1. Introduction

Bathymetric surveying of shallow waters has a great importance for coastal engineering and coastal science applications as well as shipping safety (Leu and Chang, 2005; Grilli, 1998). Especially in coastal zones intensive sediment transportation due to tidal movements, wave propagation, bottom currents, tributaries etc. cause significant temporal and spatial changes on sea bottom and made recursive surveying necessary (Zanial, 1994; Spiter and Dirks, 1987; Lyzenga, 1985, 1978). Therefore, a requirement for a practical depth estimation method arises especially for preliminary applications.

The shipboard echo sounder having been used conventionally to measure water depths gives quite accurate results for point measurements (Leu and Chang, 2005; Lyzenga, 1985). However, since it needs intensive labor, time and money, remote sensing techniques including airborne lidar measurements and optical remote sensing are preferably used in practical coastal engineering and coastal science applications. (Mas, 2004; Martin, 1993; Lyon et al., 1992). Lidar has a high accuracy in depth measurements, provided that the altitude of the measurement platform is known accurately. Its coverage is limited by maximum altitude, scan angle and position of the platform (Lyzenga, 1985, 1981). Optical remote sensing relies on passive multispectral scanner data. It uses optical characteristics of the water column to estimate water depths (Fonstad and Marcus, 2005; Lyzenga, 1978). Since multispectral scanner images can be easily obtained for different time and location, it is favored for practical bathymetric data requirements (Louchard et al., 2003).

Various depth estimation methods based on the optical remote sensing developed in the literature. For instance, Lyzenga (1978) proposed a modified exponential depth model for clear shallow waters, ignoring the internal reflection in the water column; Louchard et al. (2003) realized radiative transfer calculations to

* Corresponding author.
E-mail address: ceyhun.ozcelik@deu.edu.tr (Ö. Ceyhun).

0272-7714/$ – see front matter © 2010 Elsevier Ltd. All rights reserved.
doi:10.1016/j.ecss.2010.05.015

generate a spectral library of remote sensing reflectance and thus to classify obtained reflectance according to bottom type and water depth; Leu and Chang (2005) used two dimensional wave spectrums to estimate water depths based on the principle that while waves propagate toward shoreline, their wave lengths decrease due to decrements in water depth; Fonstad and Marcus (2005) combined remote sensing imagery and open channel flow principals to estimate water depths in clear rivers. Most of these methods are either difficult to apply or valid for only some specific conditions. Therefore, linear regression models on spectral reflectance values are generally more attractive for practical purposes because they are easy to handle as well as they can be calibrated for any area and time images.

The Single Band Algorithm (SBA) is the simplest and most widely used linear regression approach (Martin, 1993). The SBA assumes that log transformed reflectance of the pixels on a single band image are linearly correlated with water depths on those pixels. Principal Component Algorithm (PCA) or Multi-band Approach is another method that evaluates the relationship between in-situ depth measurements and log transformed reflectance values. It can evaluate multi-band images together to get better depth estimations. The PCA firstly finds the principal components (PC) of the log transformed reflectance, and then assumes that the scores of the PC are linearly correlated with water depths (Martin, 1993). Although these models provide temporal and spatial freedom and easiness in modeling, it is generally not possible to have significant linear relationships between PC scores (or single band image reflectance) and water depths, especially for the regions where environmental parameters affecting the reflectance from water column change unevenly (Leu and Chang, 2005; Fonstad and Marcus, 2005; Lyzenga, 1981). It is very complex to refine the reflectance sourced solely by depth changes from the effects of environmental factors such as bottom material, vegetation, pollution, algae cover, turbulence, tributary etc. (Hengel and Spitzer, 1991; Lyzenga, 1985). Few researchers developed different methods to able to model effects of these environmental factors (Härmä et al., 2001; Zanial, 1994; Lyon et al., 1992; Spiter and Dirks, 1987), however, there is no unique reliable method that is simple and practically applied. On the other hand, black box models, that don't need to focus on interior processes, stands as a reasonable alternative of regressive models for depth estimations via optical remote sensing.

The methodology proposed in this study use Artificial Neural Networks (ANN) to estimate water depths in shallow waters. ANN's nonlinear, sample based and model free structure allows the methodology to consider nonlinear multi-parameter relationship between reflectance from different spectral bands and water depths. Its main advantage in practice is that it can provide depth estimations without eliminating problems in optical remote sensing associated with environmental factors such as bottom material and vegetation. The proposed methodology reduces spatial and repetitive depth measurement requirement. Technical, logistical and economical difficulties on field surveys and on classical optical remote sensing make it useful especially for preliminary engineering applications. The Foca bay/Turkey was used as a test bed. Two ANN models were built. Each of these models was calibrated (trained) using Aster and Quickbird images respectively. Bathymetric maps were derived based on these models' estimations. Accuracies of results were evaluated based on two reference maps relying on different number of in-situ depth measurements. Finally, the effects of the number of the depth measurements and different band satellite images on model estimations were investigated.

2. Study area and data

The proposed ANN methodology is applied for the Foca bay, Izmir, Turkey (Fig. 1). The main economic activities in the region are fishing and tourism. Navigation is realized via the Foca port. Due to

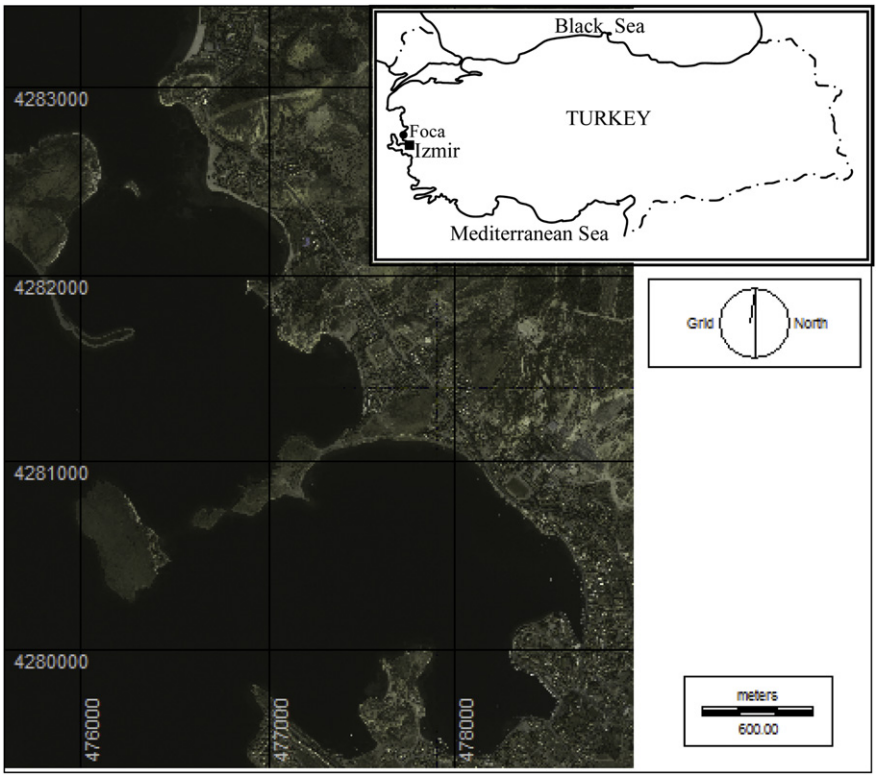

Fig. 1. The study area, Foca district.

heavy sediment transport throughout Foca shoreline, sea bottom have exposed to level changes, and thus navigation and other coastal activities such as fishing and recreation have affected negatively.

In-situ depth measurements were supplied from the surveys of the General Command of Mapping, Turkey (HGK). Aster first three band images and also Quickbird pan-sharpened first four band images were used to build depth models. Both depth measurements and satellite images were acquired in same period June–July 2005. Two reference maps were generated based on all (300)/half (150) of the depth measurements supplied, in order to see effects of the number of the depth measurements on bathymetric mapping. The distance-weighted average method was used for bathymetric map generation. The resultant maps are provided in 5 m precision to facilitate interpretations (Fig. 2).

3. Methodology

3.1. ANN modeling

ANN having a flexible information transferring structure has attracted large interest during the last years (Mas, 2004; Atkinson and Tatnall, 1997; Jain et al., 1996; Lek et al., 1996). The ability to handle nonlinear functions, estimate for unseen inputs and use observed data have made it popular (Lek et al., 1996; Civco, 1993; Freeman and Skapura, 1991). It has found wide range of application especially in environmental science, image processing, medicine and molecular biology (Mas, 2004; Atkinson and Tatnall, 1997).

Connection pattern of an artificial neural network is generally considered in two categories, feed forward and feedback (recurrent) networks (Hagan et al., 1996; Haykin, 1994). In this study multi-layer feed forward neural network (MFN) is used for depth estimations because of its simplicity in practice. In-situ depth measurements are considered as the expected output vector, and the reflectance values on each spectral band are accounted as inputs vectors. Fig. 3 shows the general structure of the ANN model proposed. Where i, j and p are, respectively, layer, node and observation numbers; n, m and N are, respectively, the numbers of layers, nodes and observations; $w_{\ell,j}$ are the network weights between the ℓth node of the $(i-1)$ th layer and jth node of the ith layer; b_j are the biases; $I_j(p)$ is jth input vector (reflectance from jth band); $T(p)$ is the calculated output vector for each epoch; $O(p)$ is the expected output vector (in-situ depth measurements). For this model, net inflow net_j to the jth node of the ith layer is defined as follows (Hagan and Menhaj, 1994; Freeman and Skapura, 1991).

$$\text{net}_j = \sum_{\ell=1}^{m} (w_{\ell,j} \times o_\ell) + b_j \tag{1}$$

where o_ℓ is the output of the ℓth node of the $(i$-1) th layer and equals to pth element of the input vectors for the first layer and to $f(\text{net}_j)$ for the other layers. $f(\text{net}_j)$ is a transfer function that transforms the net input net_j into the node outputs o_ℓ (Hagan et al., 1996). It is taken here as the log sigmoid function given in Eq. (2).

$$f(\text{net}_j) = 1/(1+\exp(-\text{net}_j)) \tag{2}$$

Model weights are calculated by using the typical performance function in Eq. (3) (Atkinson and Tatnall, 1997; Hagan and Menhaj, 1994).

$$\text{RMSE} = \sqrt{\frac{\sum_{p=1}^{N}(T(p)-O(p))^2}{N}} \tag{3}$$

If the root of mean square errors (i.e. RMSE) between calculated and observed outputs is low enough to ignore, then initial (or calculated) weights and biases are assumed as the resultant weights and biases, else the calculated error is distributed via a training algorithm to find out new weights and biases. This procedure is repeated until an acceptable RMSE is reached. Levenberg–Marquard training algorithm given in Eq. (4) is used in this study (Hagan and Menhaj, 1994).

$$x_{k+1} = x_k - \left[\mathbf{J}^{\mathrm{T}}\mathbf{J} + \mu\mathbf{I}\right]^{-1}\mathbf{J}^{\mathrm{T}}\varepsilon_k \tag{4}$$

where x_k is a vector of current weights and biases; ε and $\mathbf{J}$ are, respectively, the vector and Jacobean matrix of the network errors; μ is a scalar which indicates how to use the memory and calculation speed of the Jacobean matrix; k is iteration number; $\mathbf{I}$ is the unit matrix, and superscript T indicates transposition.

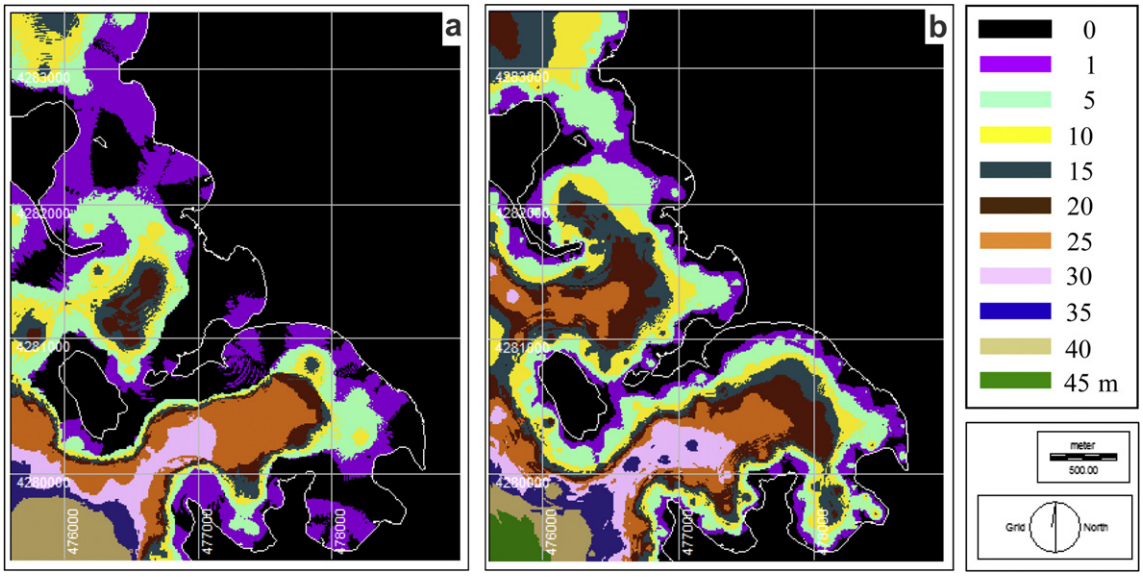

Fig. 2. Bathymetric maps generated using (a) 150, (b) 300 in-situ depth measurements.

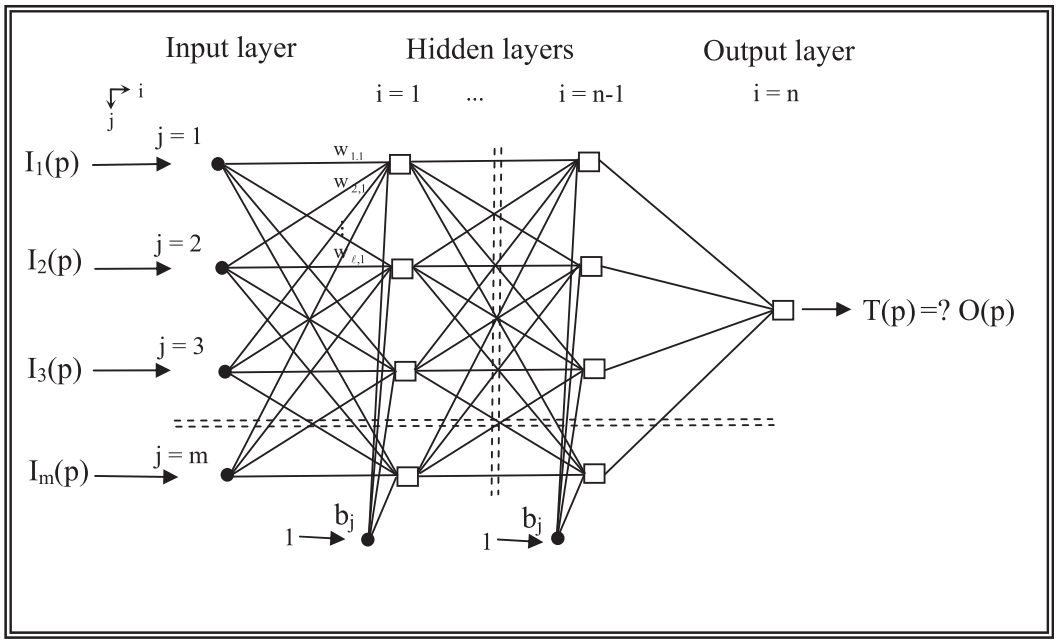

Fig. 3. Typical ANN architecture used in depth estimations.

3.2. Depth modeling and simulation

Preparation of model inputs and determination of model architecture and parameters are two important steps to model and simulate water depths in shallow waters via the ANN model proposed in Fig. 3. Model inputs, reflectance from different spectral bands and in-situ measurements, should be processed before used in the modeling. Filtering, rectifying of the input images and scaling/rescaling of the model inputs and outputs can be regarded in this manner. Model architecture is constrained by some factors such as problem to be solved, number of input factors and number of outputs required (Hagan et al., 1996). The number of the nodes in the input layer equals to the number of input spectral bands, and the number of the nodes in the output layer is naturally one since there is only one output (i.e. water depths). The number of the inner layers and nodes are determined experimentally (Freeman and Skapura, 1991) to have the best performance model. Model parameters are obtained as a result of training and testing processes. Following the preparation of model inputs and determination of model architecture and parameters, water depth simulations are made for multispectral reflectance values of required coastal points. The methodology proposed is summarized in Fig. 4.

According to Fig. 4, each band image should be first filtered to both discard the land area, clouds and ships, and decrease noise and scattering effects on input images. The land area, clouds and ships can be discarded by using a boolean filter (referred also as a binary or logical filter) while noises and scattering effects can be reduced by applying pixel based filters such as mean (low pass), Gaussian, minimum, median filters, etc. (Jain, 1989). After in-situ depth measurements and input images are transformed into same coordinate system, reflectance values corresponding to the points where there are available depth measurements (reference points) and where depth simulations will be made (key points) are extracted from input multispectral images. The key points are so selected that they do not have an individual behavior and are evenly distributed throughout considered region. To get model inputs, the input reflectance on the reference and key points and depth measurements (expected outputs) on the reference points are scaled so as to always fall within a specified range that is usable with the transfer function (see Eq. (2)). The scaled data of reference points are separated into two parts as training and testing data set. The scaled data of the key points are used in depth simulations.

Once the model inputs are prepared, model architecture and parameters can be readily determined using principles in the Section 3.1. For determined network architecture, model training and testing are conducted until an acceptable error is reached. The eventual ANN model tested is used for depth simulations on selected key and reference (if required) points. The depth estimations are obtained by rescaling network outputs. These estimates are used to interpolate a contour map or to generate a digital elevation model.

4. Application and results

Single Band Algorithm (SBA) and Principal Component Algorithm (PCA) did not provide reliable depth estimations in the study area since the bottom vegetation highly affected the reflectance from water column. Table 1 shows the coefficients of determination R^2 of the SBA and PCA models. Where R^2 designates the variance ratio of in-situ depth measurements explained by the SBA and PCA models. SBA and PCA models set for Aster images provided more reliable result than those for the Quickbird images. SBA models set for the first and third band Aster images are more reliable than the model set for second band Aster image, and also the PCA model set for the first PC is the only efficient model. The SBA model set for the Quickbird's third band image seems preferable among the models set for the Quickbird images. The PCA model set for the first PC of the Quickbird images is the only PCA model having high R^2. In overall evaluation, though some of the SBA and PCA models may be used for a course evaluation of the bathymetric structure of the region, they are not adequate for a reliable bathymetric mapping because they are not able to explain the variance of the depth variations sufficiently (see Table 1).

The ANN methodology was applied apropos to flow chart in Fig. 4. Boolean filter was used, for all band images, to discard the pixels representing the land area, clouds and vessels and thus to obtain images only from the marine environment. The Gaussian

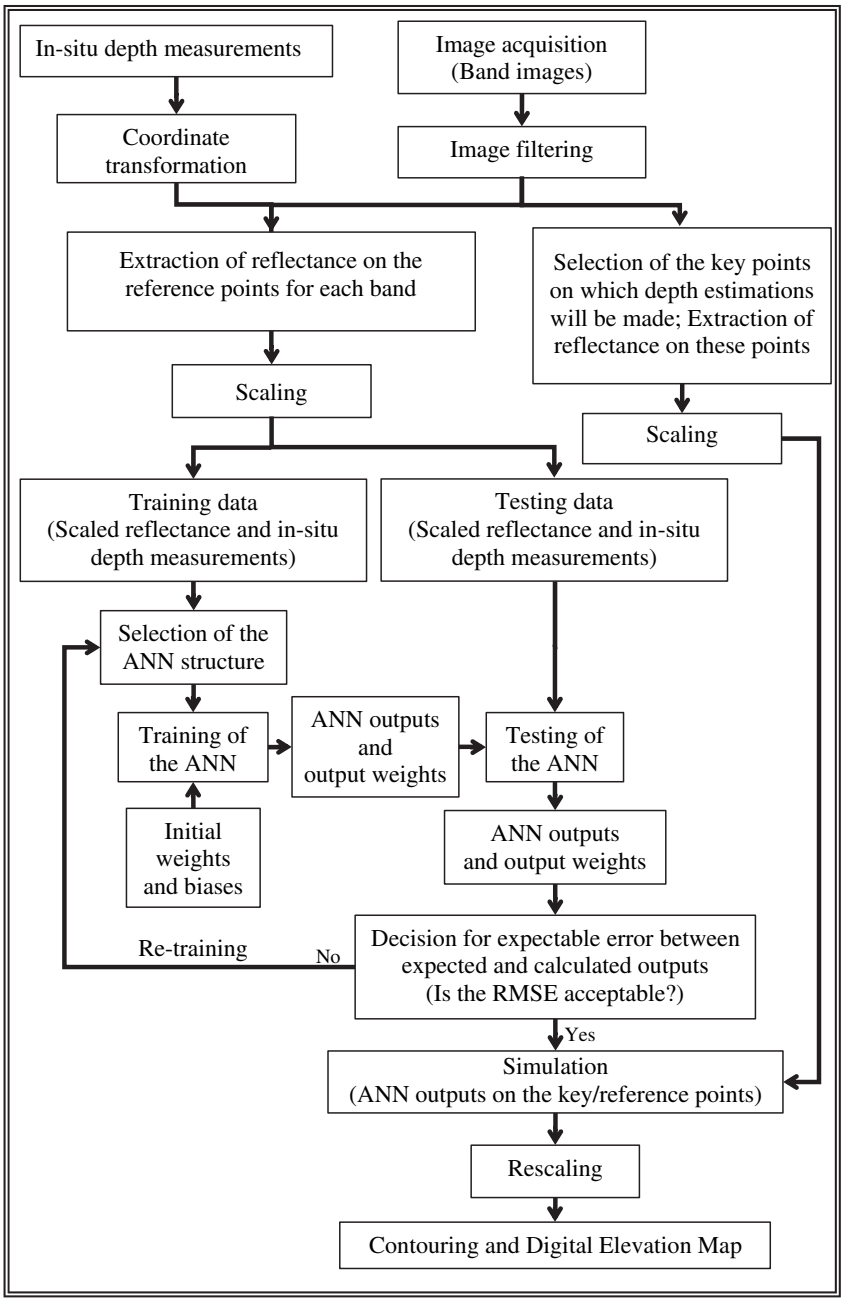

Fig. 4. Depth estimation using remote sensed images and ANN.

Table 1
The coefficients of determination for the SBA and PCA models.

Aster				Quickbird			
Single band algorithm		Principal component algorithm		Single band algorithm		Principal component algorithm	
Band number	R^2	P.C. No	R^2	Band number	R^2	P.C. No.	R^2
1	0.75	1	0.74	1	0.29	1	0.66
2	0.67	2	0.02	2	0.58	2	0.01
3	0.76	3	0.02	3	0.66	3	0.02
				4	0.51	4	0.01

5×5 filter for the Aster images and 7×7 filter for the Quickbird images were used to reduce scattering effects, noise, and problems caused by the pixels having individual reflective properties. After the filtered images and depth measurements were transformed into same reference system (UTM 35 North, WGS 84), 300 key points for the Aster model and 450 key points for the Quickbird model were specified for simulations. 300 reference points were considered in the analyses. The reflectance values on the reference/key points were extracted for all band images via a computer program written in the Visual Basic environment. Depth measurements on reference points and corresponding reflectance values were arranged into two (training and testing) data sets.

These data sets include input vectors consist of reflectance in considered spectral bands and expected output vector consist of in-situ depth measurements. Reflectance values on the key points for different spectral bands were arranged into input vectors of simulation data All input and expected output vectors constituted were scaled by $0.8 \times (R_p - R_{min})/(R_{max} - R_{min}) + 0.1$ to make them usable for the ANN analyses. Where R_p designates pth observation of the input or output vectors; R_{min} and R_{max} are the minimum and maximum observations in the vector considered, respectively.

Two ANN models, one for the Aster image inputs and the other for Quickbird image inputs were set. These models will be called hereafter as Aster and Quickbird ANN models, respectively. The architectures of the Neural Networks were determined so that the numbers of nodes and layers as well as the RMSE between calculated and measured depths would be a minimum. Two inner layers, each of which has four nodes, were used in the eventual ANN models. Since only the Aster first three band images and Quickbird first four band images have significant difference in their reflectance values on the sea surface, three and four neurons were used in the input layers respectively for Aster and Quickbird models. Levenberg–Marquardt algorithm was used to train the networks constituted. Initial weights were given randomly, and log sigmoid function was used as a transfer function. The significant epoch number, the epoch after which RMSE values begin to be level off was used to avoid over-training errors. It was calculated as 3 and 5 for Aster and Quickbird ANN models, respectively. The models trained were run for the testing data set. Regarding the Aster and Quickbird ANN models, the depth estimations obtained for the testing and training data sets were depicted against to the depth measurements (Fig. 5).

According to the results in Fig. 5(a) and (b), the calculated variance ratios explained by ANN models were accepted satisfactory. Therefore, constituted ANN models were used in depth simulations, taking the simulation data set as model input. The distance-weighted averages of the simulated depths were used to produce bathymetric maps. Resultant maps were provided in 5 m precision to facilitate comparison. Fig. 6 shows the bathymetric maps derived for the Aster and Quickbird images.

Finally, different band image combinations were used in modeling to evaluate the effects of the different bands on model performances. In these analyses, simulations were made for 15 epoch. Resultant depth estimations were compared with in-situ depth measurements. Table 2 shows the R^2 and RMSE between estimated and measured depths for each band combination used.

5. Discussion

For many coastal engineering and coastal science applications, it is very important to know bathymetry of study area. However, it is generally very difficult to get detailed information for reliable bathymetric mapping. Implementing bathymetric survey for whole study area is more expensive and time/labor consuming process. The proposed methodology presents a practical solution to estimate water depths in shallow waters via Artificial Neural Networks (ANN), using remote sensing images and sample depth measurements. Nonlinear, model free structure of ANN enables the proposed methodology to produce more accurate estimations than classical regressive methods. Areal and spatial flexibility of remote sensing images coupled with nonlinear estimation capability of ANN account for the proposed

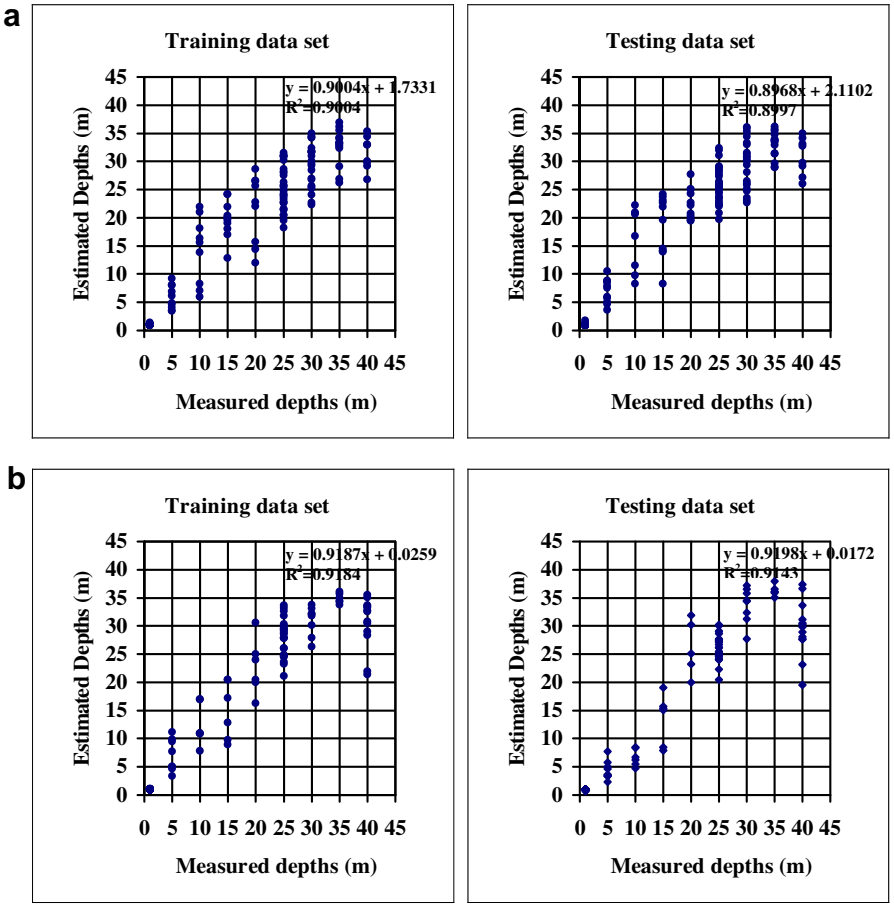

Fig. 5. Measured vs. estimated water depths, (a) Aster, (b) Quickbird ANN models.

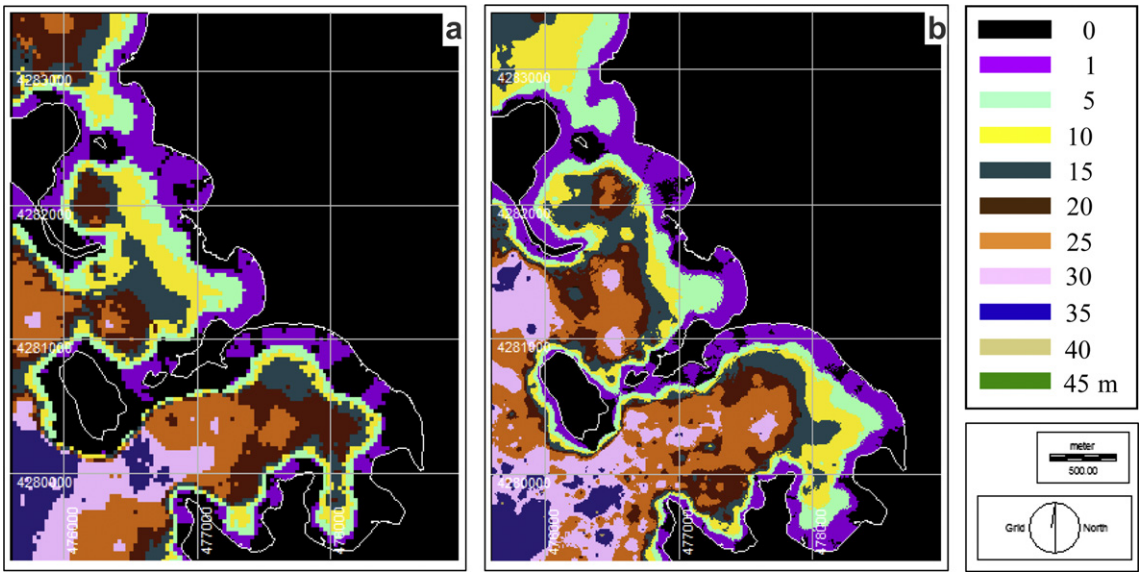

Fig. 6. Bathymetric maps derived for (a) Aster, (b) Quickbird ANN models.

methodology's prevailing advantages especially for preliminary coastal engineering studies as well as for practical scientific applications. Main advantages of the proposed methodology can be listed as below.

- provides depth estimations using raw reflectance values, without refining scattering caused by environmental factors such as bottom material and vegetation.
- allows considering nonlinear multi-parameter relationship between reflectance from different spectral bands and water depths.
- reduces spatial and repetitive depth measurement requirement.
- provides fast and practical bathymetric information.

For the analyses implemented for the study area, SBA and PCA models produced low accurate depth estimations for Aster images This may be explained by the fact that since Foca bay is subject to extensive bottom vegetation, the reflectance from water column is mainly composed of the reflectance sourced from depth changes and the reflectance sourced from bottom material. Aster and Quickbird ANN models provided more efficient estimations. Aster images have lower resolution – 15 m × 15 m – and fewer pixels therefore there is no possibility to estimates water depths for regions smaller than 225 m^2. However, when precise depth measurements can not be provided, Aster images can be conveniently used by regarding that reflectance of Aster's large pixels may produce average estimations. Aster sensor's digitations is limited by 256 values, therefore it may not account for high reliable depth estimations especially for the regions having dense bottom vegetation and turbidity. It should be noted that 256 is the full resolution of Aster's sensors, the range on the sea surface is much lower than those on the land area and changes depending on the physical and chemical properties of water column. The cleaner water will result in larger range and thus in accurate estimations (Leu and Chang, 2005; Louchard et al., 2003). Quickbird pan-sharpened images have 0.61 m × 0.61 m pixel size. Even local depth changes can be theoretically estimated. However, since the number of the pixels in a study area is larger for the Quicbird images, training and testing data sets should be larger to get reliable models, this means that more in-situ measurement is needed for the models set for Quickbird images. Correct data couples may not be easily provided for the Quickbird models since the pixel size is too small to match depth measurements to the reflectance values. On the other hand, 11 bit digitation of the Quickbird images make possible to evaluate small changes on reflective properties of the water column; therefore more precise estimations can be made by the Quickbird ANN models.

Table 2
Effects of band numbers on depth estimation performances.

Aster			Quickbird		
Bands	RMSE	R^2	Bands	RMSE	R^2
3,2,1	0.006	0.90	4,3,2,1	0.005	0.92
2,1	0.008	0.85	3,2,1	0.007	0.90
1	0.010	0.82	2,1	0.011	0.83
			1	0.021	0.67

The number of depth measurements affects remarkably the accuracy of the bathymetric mapping. This effect can be easily seen visually comparing the maps generated using different numbers of in-situ depth measurements (Fig. 2). Different depth values especially near the coast line and on the deep waters are clear. Some zero depth regions appear both on Fig. 2(a) and (b). The area of such zero depth regions is lower for Fig. 2(b) than for Fig. 2(a). There are some local depth regions on Fig. 2(b). These regions might be generated as only numerical products during map generation. Mentioned effects of the number of depth measurements on bathymetric mapping could be reduced by means of the proposed methodology. Bathymetric maps derived for the Aster and Quickbird ANN models (Fig. 6) presented more accurate and detailed bathymetric information than generated maps (i.e. Fig. 2). Due to the number and structure of the data used in bathymetric mapping, the map derived for the Quickbird image inputs (i.e. the map in Fig. 6(b)) has higher precision than the map derived for the Aster image inputs (i.e. the map in Fig. 6(a)). The area of zero depth regions is much lower for Fig. 6(b) than for Fig. 6(a). Different depth regions are clear in Fig. 6(a). The local depth regions appearing in Fig. 2(b) seems to be smoothed in Fig. 6(b). Note that reliabilities of estimations on these local regions depend highly on sampling data used in training and testing. It is seen from the Fig. 5 that depth estimations lose their effectiveness for the higher depths than 40 m since the reflectance on sea surface does not change significantly for deeper regions. This depth value can be different for other study areas, regarding water clarity.

To reveal efficiency of ANN based bathymetric mapping, the derived maps (i.e. Fig. 6(a) and (b)) and generated maps (i.e. Fig. 2 (a) and (b)) may be differenced. In-situ measurements are point

measurements contrary to the proposed methodology estimating an average depth value corresponding to the mean reflectance of the considered pixel. Unless there is no available high resolution bathymetric map for the study area, differencing may not be informative especially when images with large pixel are used in depth estimations. In this study, investigation of the effectiveness of the proposed methodology is confined with the evaluation of the training/testing results and the visual comparison of the derived and generated maps since there is no available high resolution digital bathymetric map for the region.

In the practice, bottom material, vegetation or pollution affect the reflectance from the water column, remarkably. Therefore, the input data should be representative and concurrent to build a reliable model. It is natural that the more changing properties of water column, the less reliable depth estimates; however, reliabilities of the model can be increased using large, representative data sets. Although, theoretically, simultaneous depth measurements and image acquisition are needed for modeling, data from different dated images and depth measurements may also be used under the assumption that bathymetric changes are small or homogeneous on all reference points during the date difference. However, accuracies of the results will be depended on how much depth chances have occurred on reference points between the dates of image acquisition and depth measurements. Accordingly, temporal flexibility in bathymetric mapping can be provided when depth measurements from locations where there is no significant bottom current changing bathymetry are used in modeling. Short term local pollutants will affect the model performance negatively if reference points used in training and testing and key points used in simulations are close to or under the effect of the source of pollutants. Model performance is also affected by the number of input bands used. The infrared band has no contribution for Aster model and little contribution for Quickbird model. Water depths may be estimated with moderate accuracy even using only first two bands.

6. Conclusion

Bathymetric map generation process highly depends on the number of in-situ depth measurements. Depth models provide practical solutions to increase reliability of generated bathymetric maps. However, changing bottom vegetation and material makes difficult to use classical, regressive, optic remote sensing based depth estimation methods such as SBA and PCA. The methodology proposed herein provides a useful tool for bathymetric mapping for practical purposes. Its nonlinear model free structure allows considering nonlinear relationships between multi-band image reflectance and water depths, thus more accurate depth estimations could be obtained. Since the ANN models – a black box model – do not have to consider the factors affecting the reflective properties of water column and do not have to necessarily be trained by newer in-situ measurements, the methodology can be practically applied without handling any complex reflectance separation process, and it can be reliably used for repetitive bathymetric mapping provided that there is available representative input data set.

Since the study area is subject to intensive bottom vegetation, SBA and PCA models did not provide reliable depth estimations. The proposed methodology produced quite accurate estimates. Even first two bands of both satellite images could model the bathymetry by a determination coefficient R^2 over 80%. Low digitation and spatial resolution of the Aster images facilitated data manipulation and map generation procedure. The model set for the Aster images did not provide as much reliable estimates as the model set for the Quickbird images and could not reveal precise and local depth changes; however it can be used properly when there is no need for detailed mapping. On the other hand, high resolution of the Quickbird images permitted to evaluate local depth changes. High digitation of the quickbird images made possible more precise depth estimations.

It is concluded in the study that the Artificial Neural Networks can be effectively used for bathymetric modeling. The proposed methodology can produce efficient depth estimations up to 40–45 m depending on water clarity and regardless the portion of the reflectance sourced from environmental factors. Time dependency of the bathymetric mapping may be decreased by training ANN models with newer images. Thus, the cost, labor and time spend for detailed and repeated depth measurements could be significantly reduced.

Acknowledgements

We would like to thank Dr Hüsnü ERONAT from Dokuz Eylul University The Institute of Marine Sciences and Technology for his kind helps on data provision.

References

Atkinson, P.M., Tatnall, A.R.L., 1997. Neural Networks in remote sensing. International Journal of Remote Sensing 18 (4), 699–709.
Civco, D.L., 1993. Artificial neural networks for land cover classification and mapping. International Journal of Geographic Information Systems 7 (2), 173–186.
Fonstad, M.A., Marcus, W.A., 2005. Remote sensing of stream depths with hydraulically assisted bathymetry (HAB) models. Geomorphology 72 (4), 320–339.
Freeman, J.A., Skapura, D.M., 1991. Neural Networks Algorithms, Applications and Programming Techniques. Addison-Wesley Publishing Company Inc., ISBN 0-201-51376-5.
Grilli, S.T., 1998. Depth inversion in shallow water based on nonlinear properties of shoaling periodic waves. Coastal Engineering 35 (3), 185–209.
Hagan, M.T., Demuth, H.B., Beale, M.H., 1996. Neural Network Design. PWS Publishing, Boston.
Hagan, M.T., Menhaj, M., 1994. Training feed forward networks with the Marquardt algorithm. IEEE Transactions on Neural Networks 5 (6), 989–993.
Härmä, P., Vepsäläinen, J., Hannonen, T., Pyhälahti, T., Kämäri, J., Kallio, K., Eloheimo, K., Koponen, S., 2001. Detection of water quality using simulated satellite data and semi-empirical algorithms in Finland. The Science of the Total Environmental 268, 107–121.
Haykin, S., 1994. Neural Networks: A Comprehensive Foundation. MacMillan College Publishing Co., New York.
Hengel, W.V., Spitzer, D., 1991. Multi-temporal water depth mapping by means of Landsat TM. International Journal of Remote Sensing 12 (4), 703–712.
Jain, A.K., Moa, J., Mohiuddin, K.M., 1996. Artificial Neural Networks. Theme Feature, pp. 31–44.
Jain, A.K., 1989. Fundamentals of Digital Image Processing. Prentice Hall, New Jersey.
Leu, L., Chang, H., 2005. Remotely sensing in detecting the water depths and bed load of shallow waters and their changes. Ocean Engineering 32, 1174–1198.
Lek, S., Delacoste, M., Baran, P., Dimopolos, I., Lauga, J., Aulanier, S., 1996. Application of Neural Networks to modeling nonlinear relationships in ecology. Ecological Modeling 90, 39–52.
Louchard, E.M., Reid, R.P., Stephens, F.C., Davis, C.O., Leathers, R.A., Downes, T.V., 2003. Optical remote sensing of benthic habitats and bathymetry in coastal environments at Lee stocking Island, Bahamas: a comparative spectral classification approach. Limnology and Oceanography 48 (1, 2), 511–521.
Lyzenga, D.R., 1985. Shallow-water bathymetry using combined lidar and passive multispectral scanner data. International Journal of Remote Sensing 6 (1), 15–125.
Lyzenga, D.R., 1981. Remote sensing of bottom reflectance and water attenuation parameters in shallow waters using aircraft and Landsat data. International Journal of Remote Sensing 2, 71–82.
Lyzenga, D.R., 1978. Passive remote sensing techniques for mapping water depth and bottom features. Applied Optics 17, 379–383.
Lyon, J.G., Lunetta, R.S., Williams, D.C., 1992. Airborne multi-spectral scanner data for evaluating bottom sediment types and water depths of St. Mary's River Michigan. Photogrammetric Engineering & Remote Sensing 58 (7), 951–956.
Martin, K.S., 1993. Applications in Coastal Zone, Research and Management, vol. 3. United Nations Institute for Training and Research, Geneva.
Mas, J.F., 2004. Mapping land use/cover in a tropical coastal area using satellite sensor data, GIS and Artificial Neural Networks. Estuarine, Coastal and Shelf Science 59, 219–230.
Spiter, D., Dirks, R.W.J., 1987. Bottom influence on the reflectance of the sea. International Journal of Remote Sensing 8, 279–290.
Zanial, A.J.M., 1994. New technique for enhancing the detection and classification of shallow marine habitats. Marine Technology Journal 28, 68–74.